

First observation of the decay $\Lambda_c^+ \rightarrow n K_S^0 \pi^+ \pi^0$

M. Ablikim¹, M. N. Achasov^{4,b}, P. Adlarson⁷⁵, O. Afedulidis³, X. C. Ai⁸⁰, R. Aliberti³⁵, A. Amoroso^{74A,74C}, Q. An^{71,58}, Y. Bai⁵⁷, O. Bakina³⁶, I. Balossino^{29A}, Y. Ban^{46,g}, H.-R. Bao⁶³, V. Batozskaya^{1,44}, K. Begzsuren³², N. Berger³⁵, M. Berlowski⁴⁴, M. Bertani^{28A}, D. Bettoni^{29A}, F. Bianchi^{74A,74C}, E. Bianco^{74A,74C}, A. Bortone^{74A,74C}, I. Boyko³⁶, R. A. Briere⁵, A. Brueggemann⁶⁸, H. Cai⁷⁶, X. Cai^{1,58}, A. Calcaterra^{28A}, G. F. Cao^{1,63}, N. Cao^{1,63}, S. A. Cetin^{62A}, J. F. Chang^{1,58}, W. L. Chang^{1,63}, G. R. Che⁴³, G. Chelkov^{36,a}, C. Chen⁴³, C. H. Chen⁹, Chao Chen⁵⁵, G. Chen¹, H. S. Chen^{1,63}, M. L. Chen^{1,58,63}, S. J. Chen⁴², S. L. Chen⁴⁵, S. M. Chen⁶¹, T. Chen^{1,63}, X. R. Chen^{31,63}, X. T. Chen^{1,63}, Y. B. Chen^{1,58}, Y. Q. Chen³⁴, Z. J. Chen^{25,h}, Z. Y. Chen^{1,63}, S. K. Choi^{10A}, X. Chu⁴³, G. Cibinetto^{29A}, F. Cossio^{74C}, J. J. Cui⁵⁰, H. L. Dai^{1,58}, J. P. Dai⁷⁸, A. Dbeyssi¹⁸, R. E. de Boer³, D. Dedovich³⁶, C. Q. Deng⁷², Z. Y. Deng¹, A. Denig³⁵, I. Denysenko³⁶, M. Destefanis^{74A,74C}, F. De Mori^{74A,74C}, B. Ding^{66,1}, X. X. Ding^{46,g}, Y. Ding³⁴, Y. Ding⁴⁰, J. Dong^{1,58}, L. Y. Dong^{1,63}, M. Y. Dong^{1,58,63}, X. Dong⁷⁶, M. C. Du¹, S. X. Du⁸⁰, Z. H. Duan⁴², P. Egorov^{36,a}, Y. H. Fan⁴⁵, J. Fang^{1,58}, J. Fang⁵⁹, S. S. Fang^{1,63}, W. X. Fang¹, Y. Fang¹, Y. Q. Fang^{1,58}, R. Farinelli^{29A}, L. Fava^{74B,74C}, F. Feldbauer³, G. Felici^{28A}, C. Q. Feng^{71,58}, J. H. Feng⁵⁹, Y. T. Feng^{71,58}, K. Fischer⁶⁹, M. Fritsch³, C. D. Fu¹, J. L. Fu⁶³, Y. W. Fu¹, H. Gao⁶³, Y. N. Gao^{46,g}, Yang Gao^{71,58}, S. Garbolino^{74C}, I. Garzia^{29A,29B}, L. Ge⁸⁰, P. T. Ge⁷⁶, Z. W. Ge⁴², C. Geng⁵⁹, E. M. Gersabeck⁶⁷, A. Gilman⁶, K. Goetzen¹³, L. Gong⁴⁰, W. X. Gong^{1,58}, W. Gradl³⁵, S. Gramigna^{29A,29B}, M. Greco^{74A,74C}, M. H. Gu^{1,58}, Y. T. Gu¹⁵, C. Y. Guan^{1,63}, Z. L. Guan²², A. Q. Guo^{31,63}, L. B. Guo⁴¹, M. J. Guo⁵⁰, R. P. Guo⁴⁹, Y. P. Guo^{12,f}, A. Guskov^{36,a}, J. Gutierrez²⁷, K. L. Han⁶³, T. T. Han¹, X. Q. Hao¹⁹, F. A. Harris⁶⁵, K. K. He⁵⁵, K. L. He^{1,63}, F. H. Heinsius³, C. H. Heinz³⁵, Y. K. Heng^{1,58,63}, C. Herold⁶⁰, T. Holtmann³, P. C. Hong^{12,f}, G. Y. Hou^{1,63}, X. T. Hou^{1,63}, Y. R. Hou⁶³, Z. L. Hou¹, B. Y. Hu⁵⁹, H. M. Hu^{1,63}, J. F. Hu^{56,i}, T. Hu^{1,58,63}, Y. Hu¹, G. S. Huang^{71,58}, K. X. Huang⁵⁹, L. Q. Huang^{31,63}, X. T. Huang⁵⁰, Y. P. Huang¹, T. Hussain⁷³, F. Hölzken³, N. Hüskens^{27,35}, N. in der Wiesche⁶⁸, M. Irshad^{71,58}, J. Jackson²⁷, S. Janchiv³², J. H. Jeong^{10A}, Q. Ji¹, Q. P. Ji¹⁹, W. Ji^{1,63}, X. B. Ji^{1,63}, X. L. Ji^{1,58}, Y. Y. Ji⁵⁰, X. Q. Jia⁵⁰, Z. K. Jia^{71,58}, D. Jiang^{1,63}, H. B. Jiang⁷⁶, P. C. Jiang^{46,g}, S. S. Jiang³⁹, T. J. Jiang¹⁶, X. S. Jiang^{1,58,63}, Y. Jiang⁶³, J. B. Jiao⁵⁰, J. K. Jiao³⁴, Z. Jiao²³, S. Jin⁴², Y. Jin⁶⁶, M. Q. Jing^{1,63}, X. M. Jing⁶³, T. Johansson⁷⁵, S. Kabana³³, N. Kalantar-Nayestanaki⁶⁴, X. L. Kang⁹, X. S. Kang⁴⁰, M. Kavatsyuk⁶⁴, B. C. Ke⁸⁰, V. Khachatryan²⁷, A. Khoukaz⁶⁸, R. Kiuchi¹, O. B. Kolcu^{62A}, B. Kopf³, M. Kuessner³, X. Kui^{1,63}, N. Kumar²⁶, A. Kupsc^{44,75}, W. Kühn³⁷, J. J. Lane⁶⁷, P. Larin¹⁸, L. Lavezzi^{74A,74C}, T. T. Lei^{71,58}, Z. H. Lei^{71,58}, H. Leithoff³⁵, M. Lellmann³⁵, T. Lenz³⁵, C. Li⁴⁷, C. Li⁴³, C. H. Li³⁹, Cheng Li^{71,58}, D. M. Li⁸⁰, F. Li^{1,58}, G. Li¹, H. Li^{71,58}, H. B. Li^{1,63}, H. J. Li¹⁹, H. N. Li^{56,i}, Hui Li⁴³, J. R. Li⁶¹, J. S. Li⁵⁹, Ke Li¹, L. J. Li^{1,63}, L. K. Li¹, Lei Li⁴⁸, M. H. Li⁴³, P. R. Li^{38,k}, Q. M. Li^{1,63}, Q. X. Li⁵⁰, R. Li^{17,31}, S. X. Li¹², T. Li⁵⁰, W. D. Li^{1,63}, W. G. Li¹, X. Li^{1,63}, X. H. Li^{71,58}, X. L. Li⁵⁰, Xiaoyu Li^{1,63}, Y. G. Li^{46,g}, Z. J. Li⁵⁹, Z. X. Li¹⁵, C. Liang⁴², H. Liang^{71,58}, H. Liang^{1,63}, Y. F. Liang⁵⁴, Y. T. Liang^{31,63}, G. R. Liao¹⁴, L. Z. Liao⁵⁰, Y. P. Liao^{1,63}, J. Libby²⁶, A. Limphirat⁶⁰, D. X. Lin^{31,63}, T. Lin¹, B. J. Liu¹⁵, B. X. Liu⁷⁶, C. Liu³⁴, C. X. Liu¹, F. H. Liu⁵³, Fang Liu¹, Feng Liu⁶, G. M. Liu^{56,i}, H. Liu^{38,j,k}, H. B. Liu¹⁵, H. M. Liu^{1,63}, Huanhuan Liu¹, Huihui Liu²¹, J. B. Liu^{71,58}, J. Y. Liu^{1,63}, K. Liu^{38,j,k}, K. Y. Liu⁴⁰, Ke Liu²², L. Liu^{71,58}, L. C. Liu⁴³, Lu Liu⁴³, M. H. Liu^{12,f}, P. L. Liu¹, Q. Liu⁶³, S. B. Liu^{71,58}, T. Liu^{12,f}, W. K. Liu⁴³, W. M. Liu^{71,58}, X. Liu^{38,j,k}, X. Liu³⁹, Y. Liu^{38,j,k}, Y. Liu⁸⁰, Y. B. Liu⁴³, Z. A. Liu^{1,58,63}, Z. D. Liu⁹, Z. Q. Liu⁵⁰, X. C. Lou^{1,58,63}, F. X. Lu⁵⁹, H. J. Lu²³, J. G. Lu^{1,58}, X. L. Lu¹, Y. Lu⁷, Y. P. Lu^{1,58}, Z. H. Lu^{1,63}, C. L. Luo⁴¹, M. X. Luo⁷⁹, T. Luo^{12,f}, X. L. Luo^{1,58}, X. R. Lyu⁶³, Y. F. Lyu⁴³, F. C. Ma⁴⁰, H. Ma⁷⁸, H. L. Ma¹, J. L. Ma^{1,63}, L. L. Ma⁵⁰, M. M. Ma^{1,63}, Q. M. Ma¹, R. Q. Ma^{1,63}, X. T. Ma^{1,63}, X. Y. Ma^{1,58}, Y. Ma^{46,g}, Y. M. Ma³¹, F. E. Maas¹⁸, M. Maggiora^{74A,74C}, S. Malde⁶⁹, A. Mangoni^{28B}, Y. J. Mao^{46,g}, Z. P. Mao¹, S. Marcello^{74A,74C}, Z. X. Meng⁶⁶, J. G. Messchendorp^{13,64}, G. Mezzadri^{29A}, H. Miao^{1,63}, T. J. Min⁴², R. E. Mitchell²⁷, X. H. Mo^{1,58,63}, B. Moses²⁷, N. Yu. Muchnoi^{4,b}, J. Muskalla³⁵, Y. Nefedov³⁶, F. Nerling^{18,d}, I. B. Nikolaev^{4,b}, Z. Ning^{1,58}, S. Nisar^{11,l}, Q. L. Niu^{38,j,k}, W. D. Niu⁵⁵, Y. Niu⁵⁰, S. L. Olsen⁶³, Q. Ouyang^{1,58,63}, S. Pacetti^{28B,28C}, X. Pan⁵⁵, Y. Pan⁵⁷, A. Pathak³⁴, P. Patteri^{28A}, Y. P. Pei^{71,58}, M. Pelizaeus³, H. P. Peng^{71,58}, Y. Y. Peng^{38,j,k}, K. Peters^{13,d}, J. L. Ping⁴¹, R. G. Ping^{1,63}, S. Plura³⁵, V. Prasad³³, F. Z. Qi¹, H. Qi^{71,58}, H. R. Qi⁶¹, M. Qi⁴², T. Y. Qi^{12,f}, S. Qian^{1,58}, W. B. Qian⁶³, C. F. Qiao⁶³, X. K. Qiao⁸⁰, J. J. Qin⁷², L. Q. Qin¹⁴, X. S. Qin⁵⁰, Z. H. Qin^{1,58}, J. F. Qiu¹, S. Q. Qu⁶¹, Z. H. Qu⁷², C. F. Redmer³⁵, K. J. Ren³⁹, A. Rivetti^{74C}, M. Rolo^{74C}, G. Rong^{1,63}, Ch. Rosner¹⁸, S. N. Ruan⁴³, N. Salone⁴⁴, A. Sarantsev^{36,c}, Y. Schelhaas³⁵, K. Schoenning⁷⁵, M. Scodeggio^{29A}, K. Y. Shan^{12,f}, W. Shan²⁴, X. Y. Shan^{71,58}, Z. J. Shang^{38,j,k}, J. F. Shangguan⁵⁵, L. G. Shao^{1,63}, M. Shao^{71,58}, C. P. Shen^{12,f}, H. F. Shen^{1,8}, W. H. Shen⁶³, X. Y. Shen^{1,63}, B. A. Shi⁶³, H. C. Shi^{71,58}, J. L. Shi¹², J. Y. Shi¹, Q. Q. Shi⁵⁵, R. S. Shi^{1,63}, S. Y. Shi⁷², X. Shi^{1,58}, J. Song¹⁹, T. Z. Song⁵⁹, W. M. Song^{34,1}, Y. J. Song¹², Y. X. Song^{46,g,m}, S. Sosio^{74A,74C}, S. Spataro^{74A,74C}, F. Stieler³⁵, Y. J. Su⁶³, G. B. Sun⁷⁶, G. X. Sun¹, H. Sun⁶³, H. K. Sun¹, J. F. Sun¹⁹, K. Sun⁶¹, L. Sun⁷⁶, S. S. Sun^{1,63}, T. Sun^{51,e}, W. Y. Sun³⁴, Y. Sun⁹, Y. J. Sun^{71,58}, Y. Z. Sun¹, Z. Q. Sun^{1,63}, Z. T. Sun⁵⁰, C. J. Tang⁵⁴, G. Y. Tang¹, J. Tang⁵⁹, Y. A. Tang⁷⁶, L. Y. Tao⁷², Q. T. Tao^{25,h}, M. Tat⁶⁹, J. X. Teng^{71,58}, V. Thoren⁷⁵, W. H. Tian⁵⁹, Y. Tian^{31,63}, Z. F. Tian⁷⁶, I. Uman^{62B}, Y. Wan⁵⁵, S. J. Wang⁵⁰, B. Wang¹, B. L. Wang⁶³, Bo Wang^{71,58}, D. Y. Wang^{46,g}, F. Wang⁷², H. J. Wang^{38,j,k}, J. P. Wang⁵⁰, K. Wang^{1,58}, L. L. Wang¹, M. Wang⁵⁰, Meng Wang^{1,63}, N. Y. Wang⁶³, S. Wang^{38,j,k}, S. Wang^{12,f}, T. Wang^{12,f}, T. J. Wang⁴³, W. Wang⁵⁹, W. Wang⁷², W. P. Wang^{71,58}, X. Wang^{46,g}, X. F. Wang^{38,j,k}, X. J. Wang³⁹, X. L. Wang^{12,f}, X. N. Wang¹, Y. Wang⁶¹, Y. D. Wang⁴⁵, Y. F. Wang^{1,58,63}, Y. L. Wang¹⁹, Y. N. Wang⁴⁵, Y. Q. Wang¹, Yaqian Wang¹⁷, Yi Wang⁶¹, Z. Wang^{1,58}, Z. L. Wang⁷², Z. Y. Wang^{1,63}, Ziyi Wang⁶³, D. Wei⁷⁰, D. H. Wei¹⁴, F. Weidner⁶⁸, S. P. Wen¹, Y. R. Wen³⁹, U. Wiedner³, G. Wilkinson⁶⁹, M. Wolke⁷⁵, L. Wollenberg³, C. Wu³⁹, J. F. Wu^{1,8}, L. H. Wu¹, L. J. Wu^{1,63}, X. Wu^{12,f}, X. H. Wu³⁴, Y. Wu⁷¹, Y. H. Wu⁵⁵, Y. J. Wu³¹, Z. Wu^{1,58}, L. Xia^{71,58}, X. M. Xian³⁹, B. H. Xiang^{1,63}, T. Xiang^{46,g}, D. Xiao^{38,j,k}, G. Y. Xiao⁴², S. Y. Xiao¹, Y. L. Xiao^{12,f}, Z. J. Xiao⁴¹, C. Xie⁴², X. H. Xie^{46,g}, Y. Xie⁵⁰, Y. G. Xie^{1,58}, Y. H. Xie⁶, Z. P. Xie^{71,58}, T. Y. Xing^{1,63}, C. F. Xu^{1,63}, C. J. Xu⁵⁹, G. F. Xu¹, H. Y. Xu⁶⁶, Q. J. Xu¹⁶, Q. N. Xu³⁰, W. Xu¹, W. L. Xu⁶⁶, X. P. Xu⁵⁵, Y. C. Xu⁷⁷, Z. P. Xu⁴²,

Z. S. Xu⁶³, F. Yan^{12,f}, L. Yan^{12,f}, W. B. Yan^{71,58}, W. C. Yan⁸⁰, X. Q. Yan¹, H. J. Yang^{51,e}, H. L. Yang³⁴, H. X. Yang¹, Tao Yang¹, Y. Yang^{12,f}, Y. F. Yang⁴³, Y. X. Yang^{1,63}, Yifan Yang^{1,63}, Z. W. Yang^{38,j,k}, Z. P. Yao⁵⁰, M. Ye^{1,58}, M. H. Ye⁸, J. H. Yin¹, Z. Y. You⁵⁹, B. X. Yu^{1,58,63}, C. X. Yu⁴³, G. Yu^{1,63}, J. S. Yu^{25,h}, T. Yu⁷², X. D. Yu^{46,g}, Y. C. Yu⁸⁰, C. Z. Yuan^{1,63}, J. Yuan³⁴, L. Yuan², S. C. Yuan¹, Y. Yuan^{1,63}, Z. Y. Yuan⁵⁹, C. X. Yue³⁹, A. A. Zafar⁷³, F. R. Zeng⁵⁰, S. H. Zeng⁷², X. Zeng^{12,f}, Y. Zeng^{25,h}, Y. J. Zeng⁵⁹, Y. J. Zeng^{1,63}, X. Y. Zhai³⁴, Y. C. Zhai⁵⁰, Y. H. Zhan⁵⁹, A. Q. Zhang^{1,63}, B. L. Zhang^{1,63}, B. X. Zhang¹, D. H. Zhang⁴³, G. Y. Zhang¹⁹, H. Zhang⁷¹, H. C. Zhang^{1,58,63}, H. H. Zhang⁵⁹, H. H. Zhang³⁴, H. Q. Zhang^{1,58,63}, H. Y. Zhang^{1,58}, J. Zhang⁸⁰, J. Zhang⁵⁹, J. J. Zhang⁵², J. L. Zhang²⁰, J. Q. Zhang⁴¹, J. W. Zhang^{1,58,63}, J. X. Zhang^{38,j,k}, J. Y. Zhang¹, J. Z. Zhang^{1,63}, Jianyu Zhang⁶³, L. M. Zhang⁶¹, Lei Zhang⁴², P. Zhang^{1,63}, Q. Y. Zhang^{39,80}, R. Y. Zhang^{38,j,k}, Shuihan Zhang^{1,63}, Shulei Zhang^{25,h}, X. D. Zhang⁴⁵, X. M. Zhang¹, X. Y. Zhang⁵⁰, Y. Zhang⁷², Y. T. Zhang⁸⁰, Y. H. Zhang^{1,58}, Y. M. Zhang³⁹, Yan Zhang^{71,58}, Yao Zhang¹, Z. D. Zhang¹, Z. H. Zhang¹, Z. L. Zhang³⁴, Z. Y. Zhang⁷⁶, Z. Y. Zhang⁴³, G. Zhao¹, J. Y. Zhao^{1,63}, J. Z. Zhao^{1,58}, Lei Zhao^{71,58}, Ling Zhao¹, M. G. Zhao⁴³, R. P. Zhao⁶³, S. J. Zhao⁸⁰, Y. B. Zhao^{1,58}, Y. X. Zhao^{31,63}, Z. G. Zhao^{71,58}, A. Zhemchugov^{36,a}, B. Zheng⁷², J. P. Zheng^{1,58}, W. J. Zheng^{1,63}, Y. H. Zheng⁶³, B. Zhong⁴¹, X. Zhong⁵⁹, H. Zhou⁵⁰, J. Y. Zhou³⁴, L. P. Zhou^{1,63}, X. Zhou⁷⁶, X. K. Zhou⁶, X. R. Zhou^{71,58}, X. Y. Zhou³⁹, Y. Z. Zhou^{12,f}, J. Zhu⁴³, K. Zhu¹, K. J. Zhu^{1,58,63}, L. Zhu³⁴, L. X. Zhu⁶³, S. H. Zhu⁷⁰, S. Q. Zhu⁴², T. J. Zhu^{12,f}, W. J. Zhu^{12,f}, Y. C. Zhu^{71,58}, Z. A. Zhu^{1,63}, J. H. Zou¹, J. Zu^{71,58}

(BESIII Collaboration)

¹ *Institute of High Energy Physics, Beijing 100049, People's Republic of China*

² *Beihang University, Beijing 100191, People's Republic of China*

³ *Bochum Ruhr-University, D-44780 Bochum, Germany*

⁴ *Budker Institute of Nuclear Physics SB RAS (BINP), Novosibirsk 630090, Russia*

⁵ *Carnegie Mellon University, Pittsburgh, Pennsylvania 15213, USA*

⁶ *Central China Normal University, Wuhan 430079, People's Republic of China*

⁷ *Central South University, Changsha 410083, People's Republic of China*

⁸ *China Center of Advanced Science and Technology, Beijing 100190, People's Republic of China*

⁹ *China University of Geosciences, Wuhan 430074, People's Republic of China*

¹⁰ *Chung-Ang University, Seoul, 06974, Republic of Korea*

¹¹ *COMSATS University Islamabad, Lahore Campus, Defence Road, Off Raiwind Road, 54000 Lahore, Pakistan*

¹² *Fudan University, Shanghai 200433, People's Republic of China*

¹³ *GSI Helmholtzcentre for Heavy Ion Research GmbH, D-64291 Darmstadt, Germany*

¹⁴ *Guangxi Normal University, Guilin 541004, People's Republic of China*

¹⁵ *Guangxi University, Nanning 530004, People's Republic of China*

¹⁶ *Hangzhou Normal University, Hangzhou 310036, People's Republic of China*

¹⁷ *Hebei University, Baoding 071002, People's Republic of China*

¹⁸ *Helmholtz Institute Mainz, Staudinger Weg 18, D-55099 Mainz, Germany*

¹⁹ *Henan Normal University, Xinxiang 453007, People's Republic of China*

²⁰ *Henan University, Kaifeng 475004, People's Republic of China*

²¹ *Henan University of Science and Technology, Luoyang 471003, People's Republic of China*

²² *Henan University of Technology, Zhengzhou 450001, People's Republic of China*

²³ *Huangshan College, Huangshan 245000, People's Republic of China*

²⁴ *Hunan Normal University, Changsha 410081, People's Republic of China*

²⁵ *Hunan University, Changsha 410082, People's Republic of China*

²⁶ *Indian Institute of Technology Madras, Chennai 600036, India*

²⁷ *Indiana University, Bloomington, Indiana 47405, USA*

²⁸ *INFN Laboratori Nazionali di Frascati, (A)INFN Laboratori Nazionali di Frascati, I-00044, Frascati, Italy; (B)INFN Sezione di Perugia, I-06100, Perugia, Italy; (C)University of Perugia, I-06100, Perugia, Italy*

²⁹ *INFN Sezione di Ferrara, (A)INFN Sezione di Ferrara, I-44122, Ferrara, Italy; (B)University of Ferrara, I-44122, Ferrara, Italy*

³⁰ *Inner Mongolia University, Hohhot 010021, People's Republic of China*

³¹ *Institute of Modern Physics, Lanzhou 730000, People's Republic of China*

³² *Institute of Physics and Technology, Peace Avenue 54B, Ulaanbaatar 13330, Mongolia*

³³ *Instituto de Alta Investigación, Universidad de Tarapacá, Casilla 7D, Arica 1000000, Chile*

³⁴ *Jilin University, Changchun 130012, People's Republic of China*

³⁵ *Johannes Gutenberg University of Mainz, Johann-Joachim-Becher-Weg 45, D-55099 Mainz, Germany*

³⁶ *Joint Institute for Nuclear Research, 141980 Dubna, Moscow region, Russia*

³⁷ *Justus-Liebig-Universität Giessen, II. Physikalisches Institut, Heinrich-Buff-Ring 16, D-35392 Giessen, Germany*

³⁸ *Lanzhou University, Lanzhou 730000, People's Republic of China*

³⁹ *Liaoning Normal University, Dalian 116029, People's Republic of China*

⁴⁰ *Liaoning University, Shenyang 110036, People's Republic of China*

⁴¹ *Nanjing Normal University, Nanjing 210023, People's Republic of China*

⁴² *Nanjing University, Nanjing 210093, People's Republic of China*

⁴³ *Nankai University, Tianjin 300071, People's Republic of China*

⁴⁴ *National Centre for Nuclear Research, Warsaw 02-093, Poland*

- ⁴⁵ North China Electric Power University, Beijing 102206, People's Republic of China
- ⁴⁶ Peking University, Beijing 100871, People's Republic of China
- ⁴⁷ Qufu Normal University, Qufu 273165, People's Republic of China
- ⁴⁸ Renmin University of China, Beijing 100872, People's Republic of China
- ⁴⁹ Shandong Normal University, Jinan 250014, People's Republic of China
- ⁵⁰ Shandong University, Jinan 250100, People's Republic of China
- ⁵¹ Shanghai Jiao Tong University, Shanghai 200240, People's Republic of China
- ⁵² Shanxi Normal University, Linfen 041004, People's Republic of China
- ⁵³ Shanxi University, Taiyuan 030006, People's Republic of China
- ⁵⁴ Sichuan University, Chengdu 610064, People's Republic of China
- ⁵⁵ Soochow University, Suzhou 215006, People's Republic of China
- ⁵⁶ South China Normal University, Guangzhou 510006, People's Republic of China
- ⁵⁷ Southeast University, Nanjing 211100, People's Republic of China
- ⁵⁸ State Key Laboratory of Particle Detection and Electronics, Beijing 100049, Hefei 230026, People's Republic of China
- ⁵⁹ Sun Yat-Sen University, Guangzhou 510275, People's Republic of China
- ⁶⁰ Suranaree University of Technology, University Avenue 111, Nakhon Ratchasima 30000, Thailand
- ⁶¹ Tsinghua University, Beijing 100084, People's Republic of China
- ⁶² Turkish Accelerator Center Particle Factory Group, (A)Istinye University, 34010, Istanbul, Turkey; (B)Near East University, Nicosia, North Cyprus, 99138, Mersin 10, Turkey
- ⁶³ University of Chinese Academy of Sciences, Beijing 100049, People's Republic of China
- ⁶⁴ University of Groningen, NL-9747 AA Groningen, The Netherlands
- ⁶⁵ University of Hawaii, Honolulu, Hawaii 96822, USA
- ⁶⁶ University of Jinan, Jinan 250022, People's Republic of China
- ⁶⁷ University of Manchester, Oxford Road, Manchester, M13 9PL, United Kingdom
- ⁶⁸ University of Muenster, Wilhelm-Klemm-Strasse 9, 48149 Muenster, Germany
- ⁶⁹ University of Oxford, Keble Road, Oxford OX13RH, United Kingdom
- ⁷⁰ University of Science and Technology Liaoning, Anshan 114051, People's Republic of China
- ⁷¹ University of Science and Technology of China, Hefei 230026, People's Republic of China
- ⁷² University of South China, Hengyang 421001, People's Republic of China
- ⁷³ University of the Punjab, Lahore-54590, Pakistan
- ⁷⁴ University of Turin and INFN, (A)University of Turin, I-10125, Turin, Italy; (B)University of Eastern Piedmont, I-15121, Alessandria, Italy; (C)INFN, I-10125, Turin, Italy
- ⁷⁵ Uppsala University, Box 516, SE-75120 Uppsala, Sweden
- ⁷⁶ Wuhan University, Wuhan 430072, People's Republic of China
- ⁷⁷ Yantai University, Yantai 264005, People's Republic of China
- ⁷⁸ Yunnan University, Kunming 650500, People's Republic of China
- ⁷⁹ Zhejiang University, Hangzhou 310027, People's Republic of China
- ⁸⁰ Zhengzhou University, Zhengzhou 450001, People's Republic of China
- ^a Also at the Moscow Institute of Physics and Technology, Moscow 141700, Russia
- ^b Also at the Novosibirsk State University, Novosibirsk, 630090, Russia
- ^c Also at the NRC "Kurchatov Institute", PNPI, 188300, Gatchina, Russia
- ^d Also at Goethe University Frankfurt, 60323 Frankfurt am Main, Germany
- ^e Also at Key Laboratory for Particle Physics, Astrophysics and Cosmology, Ministry of Education; Shanghai Key Laboratory for Particle Physics and Cosmology; Institute of Nuclear and Particle Physics, Shanghai 200240, People's Republic of China
- ^f Also at Key Laboratory of Nuclear Physics and Ion-beam Application (MOE) and Institute of Modern Physics, Fudan University, Shanghai 200443, People's Republic of China
- ^g Also at State Key Laboratory of Nuclear Physics and Technology, Peking University, Beijing 100871, People's Republic of China
- ^h Also at School of Physics and Electronics, Hunan University, Changsha 410082, China
- ⁱ Also at Guangdong Provincial Key Laboratory of Nuclear Science, Institute of Quantum Matter, South China Normal University, Guangzhou 510006, China
- ^j Also at MOE Frontiers Science Center for Rare Isotopes, Lanzhou University, Lanzhou 730000, People's Republic of China
- ^k Also at Lanzhou Center for Theoretical Physics, Lanzhou University, Lanzhou 730000, People's Republic of China
- ^l Also at the Department of Mathematical Sciences, IBA, Karachi 75270, Pakistan
- ^m Also at Ecole Polytechnique Federale de Lausanne (EPFL), CH-1015 Lausanne, Switzerland

(Dated: April 1, 2024)

Based on 4.5 fb^{-1} of e^+e^- collision data accumulated at center-of-mass energies between 4599.53 MeV and 4698.82 MeV with the BESIII detector, the decay $\Lambda_c^+ \rightarrow n K_S^0 \pi^+ \pi^0$ is observed for the first time with a significance of 9.2σ . The branching fraction is measured to be $(0.85 \pm 0.13 \pm 0.03)\%$, where the first uncertainty is statistical and the second systematic, which differs from the theoretical prediction based on isospin by 4.4σ . This indicates that there may be resonant contributions or some unknown dynamics in this decay.

INTRODUCTION

Experimental studies of charmed baryon decays provide important information on the strong and weak interactions in the environment of heavy quarks. The lightest charmed baryon, Λ_c^+ , was first observed in e^+e^- annihilation at the Mark II experiment [1]. So far, 70% of the Λ_c^+ decays have been observed [2, 3], of which the total branching fraction (BF) of the decays involving a neutron is $(32.4 \pm 1.7)\%$ [4]. To deeply understand the properties of non-perturbative quantum chromodynamics, studies of multi-body hadronic decays which include potential intermediate processes are needed. Recently, the BFs of the Cabibbo-favored four body decays $\Lambda_c^+ \rightarrow pK^-\pi^+\pi^0$ [5], $\Lambda_c^+ \rightarrow nK^-\pi^+\pi^+$ [6], and $\Lambda_c^+ \rightarrow pK_S^0\pi^+\pi^-$ [5] were measured to be $(4.53 \pm 0.38)\%$, $(1.90 \pm 0.12)\%$, and $(1.53 \pm 0.14)\%$, respectively. However, the isospin-related decay $\Lambda_c^+ \rightarrow nK_S^0\pi^+\pi^0$ has not been observed yet.

Theoretically, the decay amplitude of Λ_c^+ consists of factorizable and non-factorizable contributions [7, 8]. It is known that the non-factorizable contribution is negligible compared to the factorizable one in describing the non-leptonic weak decays of charmed mesons [9]. However, the contributions are different in Λ_c^+ decays, where the W -exchange diagram manifesting a pole diagram is no longer subject to helicity and color suppression [10]. As shown in Fig. 1, the $\Lambda_c^+ \rightarrow nK_S^0\pi^+\pi^0$ decay proceeds through external and internal W -emission processes, where the dynamics includes both factorizable and non-factorizable contributions. There has been much progress in the theoretical and experimental studies of the two-body decays of the Λ_c^+ [11]. However, due to possible intermediate resonances, the dynamics of multi-body decays of Λ_c^+ is more complex, and theoretical calculations are not reliable yet. The decay $\Lambda_c^+ \rightarrow nK_S^0\pi^+\pi^0$ is dominated by the weak interaction process $c \rightarrow sud$. A phenomenological model based on isospin [12] predicts a BF for this decay of $(1.54 \pm 0.08)\%$ and further relates the BFs for all $N\bar{K}\pi\pi$ final states.

In this paper, we report the first observation of $\Lambda_c^+ \rightarrow nK_S^0\pi^+\pi^0$ based on the data samples accumulated at center-of-mass (c.m.) energies between 4599.53 MeV and 4698.82 MeV with the BESIII detector. These data samples correspond to an integrated luminosity of 4.5 fb^{-1} [13–16], as listed in Table I. Due to the energy being just above the threshold of $\Lambda_c^+\bar{\Lambda}_c^-$ pair production, the $\Lambda_c^+\bar{\Lambda}_c^-$ pairs are generated without other accompanied hadrons, which makes it feasible to apply the double-tag (DT) method [17] and reconstruct the neutron with missing neutron mass technique. The Λ_c^+ is reconstructed by recoiling against the single-tag (ST) candidate $\bar{\Lambda}_c^-$ at these c.m. energies, and an event containing an ST $\bar{\Lambda}_c^-$ and a signal Λ_c^+ is referred to as a DT candidate. Charge-conjugated decays are implied throughout this paper.

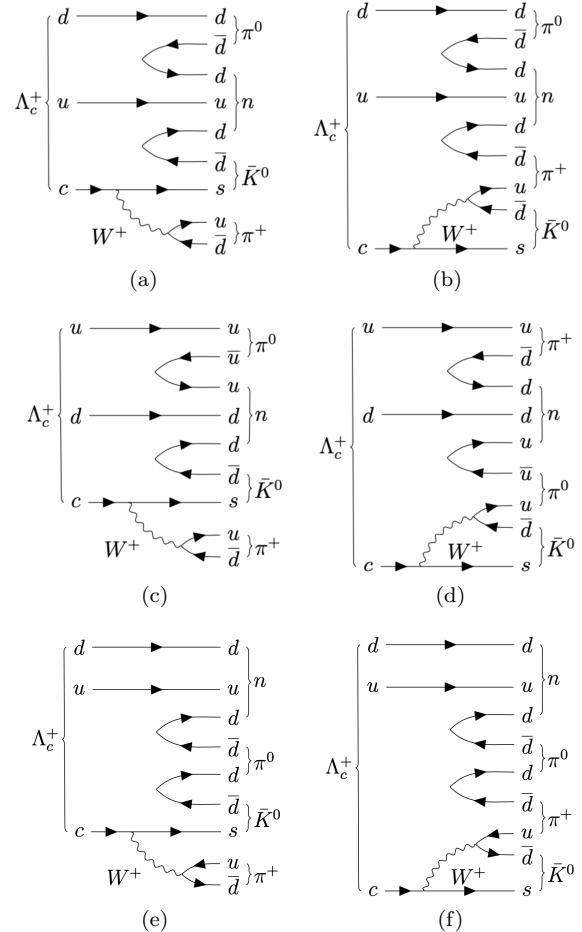


Figure 1. Feynman diagrams for $\Lambda_c^+ \rightarrow nK_S^0\pi^+\pi^0$: (a),(c),(e) External W -emission; (b),(d),(f) Internal W -emission.

Table I. The c.m. energies and integrated luminosities for each data sample, where the first uncertainties are statistical, and the second ones are systematic.

\sqrt{s} (MeV)	Luminosity (pb^{-1})
$4599.53 \pm 0.07 \pm 0.74$	$586.90 \pm 0.10 \pm 3.90$
$4611.86 \pm 0.12 \pm 0.32$	$103.65 \pm 0.05 \pm 0.55$
$4628.00 \pm 0.06 \pm 0.32$	$521.53 \pm 0.11 \pm 2.76$
$4640.91 \pm 0.06 \pm 0.38$	$551.65 \pm 0.12 \pm 2.92$
$4661.24 \pm 0.06 \pm 0.29$	$529.43 \pm 0.12 \pm 2.81$
$4681.92 \pm 0.08 \pm 0.29$	$1667.39 \pm 0.21 \pm 8.84$
$4698.82 \pm 0.10 \pm 0.39$	$535.54 \pm 0.12 \pm 2.84$

BESIII EXPERIMENT AND MONTE CARLO SIMULATION

The BESIII detector [18] records symmetric e^+e^- collisions provided by the BEPCII storage ring [19] in the c.m. energy ranging from 2.0 to 4.95 GeV, with a peak luminosity of $1 \times 10^{33} \text{ cm}^{-2}\text{s}^{-1}$ achieved at $\sqrt{s} = 3.773$ GeV. BESIII has collected large data samples in this energy region [20]. The cylindrical core of the BESIII de-

tector covers 93% of the full solid angle and consists of a helium-based multilayer drift chamber (MDC), a plastic scintillator time-of-flight system (TOF), and a CsI(Tl) electromagnetic calorimeter (EMC), which are all enclosed in a superconducting solenoidal magnet providing a 1.0 T magnetic field. The solenoid is supported by an octagonal flux-return yoke with resistive plate counter muon identification modules interleaved with steel. The charged-particle momentum resolution at 1 GeV/c is 0.5%, and the resolution of energy deposited (dE/dx) is 6% for electrons from Bhabha scattering. The EMC measures photon energies with a resolution of 2.5% (5%) at 1 GeV in the barrel (end-cap) region. The time resolution in the TOF barrel region is 68 ps, while that in the end-cap region is 110 ps. The end cap TOF system was upgraded in 2015 using multigap resistive plate chamber technology, providing a time resolution of 60 ps. About 87% of the data used in this analysis benefits from this upgrade. More detailed descriptions can be found in Refs. [18, 19].

Monte-Carlo (MC) simulated samples are used to determine the detection efficiencies, optimize selection criteria, and study backgrounds. The simulation is carried out with a GEANT4-based [21] package including the geometric description of the BESIII detector and the detector response [22], and models the beam-energy spread and initial-state radiation (ISR) in the e^+e^- annihilation with the generator KKMC [23]. Final-state radiation from charged final-state particles is incorporated using the PHOTOS package [24]. The inclusive MC samples include the production of $\Lambda_c^+\bar{\Lambda}_c^-$ pairs, open-charmed mesons, ISR production of vector charmonium(-like) states, and continuum processes, which are used to determine ST efficiencies, analyze backgrounds, and extract background shapes. Known decay modes are modeled with EVTGEN [25, 26] using BFs taken from the Particle Data Group (PDG) [2]. The remaining unknown charmonium decays are modeled with LUNDCHARM [27, 28]. The angular distribution of $e^+e^- \rightarrow \Lambda_c^+\bar{\Lambda}_c^-$ is generated as $1 + \alpha \cos^2 \theta_{\Lambda_c^+}$, where $\theta_{\Lambda_c^+}$ is the polar angle between the Λ_c^+ and the positron beam in the c.m. frame, and α is the angular parameter of Λ_c^+ production, which is different at the seven c.m. energy points [29]. The signal MC sample consists of the exclusive process where the $\bar{\Lambda}_c^-$ decays to eleven ST tag modes and the Λ_c^+ decays to $nK_S^0\pi^+\pi^0$, with $K_S^0 \rightarrow \pi^+\pi^-$ and $\pi^0 \rightarrow \gamma\gamma$, which is used to determine DT efficiencies and extract signal shapes. The $\Lambda_c^+ \rightarrow nK_S^0\pi^+\pi^0$ signal MC sample is simulated using a phase space (PHSP) model which then has the four daughter (K_S^0, n, π^+, π^0) momentum and the $n\pi^+\pi^0$ invariant mass distributions weighted to match those of data.

EVENT SELECTION

The selection criteria of the ST candidates $\bar{\Lambda}_c^- \rightarrow \bar{p}K_S^0, \bar{p}K^+\pi^-, \bar{p}K^+\pi^-\pi^0, \bar{\Lambda}\pi^-, \bar{\Lambda}\pi^-\pi^0, \bar{\Sigma}^-\pi^-\pi^+, \bar{p}K_S^0\pi^0, \bar{\Sigma}^-\pi^0, \bar{\Sigma}^0\pi^-, \bar{\Lambda}\pi^-\pi^+\pi^-,$ and $\bar{p}K_S^0\pi^-\pi^+$ are the same as Ref. [6]. The ST $\bar{\Lambda}_c^-$ is identified with the beam-constrained mass $M_{BC} \equiv \sqrt{E_{\text{beam}}^2/c^4 - p_{\Lambda_c}^2/c^2}$, where E_{beam} is the beam energy and p_{Λ_c} is the measured momentum of the $\bar{\Lambda}_c^-$ in the c.m. system of e^+e^- collision. Figure 2 shows the M_{BC} distributions of various ST modes for the data sample at $\sqrt{s} = 4681.92$ MeV; clear $\bar{\Lambda}_c^-$ signals are observed in each mode. The signal and sideband regions for the ST candidates are defined as (2.280, 2.296) GeV/ c^2 and (2.250, 2.270) GeV/ c^2 , respectively. Candidates in the signal region are used for the further DT reconstruction, and those in the sideband region are used to estimate the background contribution.

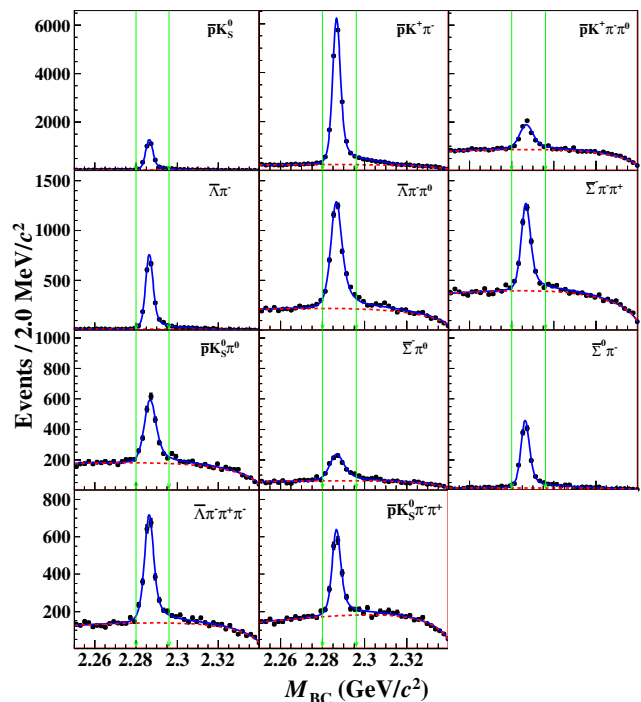


Figure 2. The M_{BC} distributions of the ST modes for the data sample at $\sqrt{s} = 4681.92$ MeV. The points with error bars represent data. The blue solid curves indicate the fit results, the red dashed curves describe the background shapes, and the green lines are defined as signal region.

The $K_S^0(\pi^+\pi^-), \pi^+, \pi^0(\gamma\gamma)$ from the signal side decay $\Lambda_c^+ \rightarrow nK_S^0\pi^+\pi^0$ are reconstructed with the following criteria. Charged tracks detected in the MDC are required to be within a polar angle (θ) range of $|\cos \theta| < 0.93$, where θ is defined with respect to the z -axis which is the symmetry axis of the MDC. The K_S^0 candidate is reconstructed from two oppositely charged tracks satis-

fying $|V_z| < 20$ cm, where V_z denotes the distance to the interaction point (IP) along z -axis. The two charged tracks are assigned as $\pi^+\pi^-$ without imposing further particle identification (PID) criteria to improve the K_S^0 reconstruction efficiency. They are required to originate from a common vertex. The decay length (L) of the K_S^0 candidate is required to be greater than twice the vertex resolution (σ_L) away from IP, *i.e.*, $L/\sigma_L > 2$. If there are multiple K_S^0 candidates, the one with the largest L/σ_L is retained.

Apart from the K_S^0 candidate, there is one other charged track: the π^+ from the Λ_c^+ decay. The distance of closest approach to the IP for this track must be less than 10 cm along the z -axis, $|V_z| < 10$ cm, and less than 1 cm in the transverse plane, $|V_{xy}| < 1$ cm. The PID for this track combines the measurements of dE/dx in the MDC and the flight time in the TOF to form likelihoods $\mathcal{L}(h)$ ($h = p, K, \pi$) for each hadron (h) hypothesis. The track needs to satisfy $\mathcal{L}(\pi) > \mathcal{L}(K)$.

The photon candidates are identified as showers in the EMC. The deposited energy of each shower must be more than 25 MeV in the barrel region ($|\cos\theta| < 0.80$) and more than 50 MeV in the end cap region ($0.86 < |\cos\theta| < 0.92$) of the EMC. To exclude showers that originate from the charged track radiation, the angle subtended by the EMC shower and the position of the closest charged track at the EMC must be greater than 10 degrees as measured from the IP. To suppress electronic noise and showers unrelated to the event, the difference between the EMC time and the event start time is required to be within [0, 700] ns. The invariant mass $m_{\gamma\gamma}$ of the two photons from the π^0 decay has to satisfy $0.115 < m_{\gamma\gamma} < 0.150$ GeV/ c^2 . In addition, a one-constraint (1C) kinematic fit is performed to constrain $m_{\gamma\gamma}$ to the π^0 known mass [2]. The fit chi-squared, χ_{1C}^2 , is required to be less than 200. If there are more than one π^0 candidates, the one with the smallest χ_{1C}^2 is retained.

Considering that the neutron is difficult to detect, it is reconstructed with the missing-mass technique, using the kinematic variable $M(n) = \sqrt{E_{\text{miss}}^2/c^4 - |\vec{p}_{\text{miss}}|^2/c^2}$. Here, the E_{miss} and \vec{p}_{miss} are calculated by $E_{\text{miss}} = E_{\text{beam}} - E_{\text{rec}}$ and $\vec{p}_{\text{miss}} = \vec{p}_{\Lambda_c^+} - \vec{p}_{\text{rec}}$, where E_{rec} (\vec{p}_{rec}) is the sum of the energies (vector momenta) of the reconstructed K_S^0 , π^+ and π^0 in the e^+e^- c.m. system. The Λ_c^+ momentum $\vec{p}_{\Lambda_c^+}$ is derived by $\vec{p}_{\Lambda_c^+} = -\hat{p}_{\text{tag}} \sqrt{E_{\text{beam}}^2/c^2 - m_{\Lambda_c^+}^2 c^2}$, where \hat{p}_{tag} is the unit vector of the $\bar{\Lambda}_c^-$ momentum direction and $m_{\Lambda_c^+}$ is the Λ_c^+ nominal mass [2].

A study of the inclusive MC sample shows that the peaking backgrounds are mainly from $\Lambda_c^+ \rightarrow \Sigma^-(n\pi^-)\pi^+\pi^+\pi^0$, $\Lambda(n\pi^0)\pi^+\pi^-\pi^+$, and $\Sigma^+(n\pi^+)\omega(\pi^+\pi^-\pi^0)$. In order to remove these peaking backgrounds, the difference of the invariant masses $M(n\pi^-) - M(n)$ is required to be outside the interval (0.22, 0.27) GeV/ c^2 and $M(n\pi^0) - M(n)$ must be larg-

er than 0.20 GeV/ c^2 . Also, both values of $M(n\pi^+) - M(n)$ are required to lie outside of the interval of (0.23, 0.28) GeV/ c^2 , where the two $M(n\pi^+)$ combinations include the π^+ from either the Λ_c^+ or the K_S^0 . Here, $M(n\pi^+)$, $M(n\pi^-)$, and $M(n\pi^0)$ denote the invariant masses of the missing neutron and π^+ , π^- , and π^0 , respectively. Figure 3 shows $M(n)$ and $M(\pi^+\pi^-)$ distributions of signal MC in the signal region after applying all the above selections.

ABSOLUTE BF MEASUREMENT

The signal yield of $\Lambda_c^+ \rightarrow nK_S^0\pi^+\pi^0$ is obtained by performing a two-dimensional (2D) unbinned maximum likelihood fit to the $M(n)$ and $M(\pi^+\pi^-)$ spectra of the candidates combined from the data sets at seven c.m. energies shown in Fig. 4. The signal shapes (f_{sig}) are determined from signal MC samples convolved with a 2D Gaussian function, which accounts for the difference in mass resolution between data and MC simulation. This 2D Gaussian function is extracted by using two Gaussian functions to fit the 2D $M(n)$ and $M(\pi^+\pi^-)$ spectra in data with the correlation between them taken into account.

In the fit, the probability density functions of the signal and sideband regions are constructed as:

$$f_{\text{signal}} = N_{\text{sig}} \cdot f_{\text{sig}} + N_{\Lambda_c^+ \text{ bkg}} \cdot f_{\Lambda_c^+ \text{ bkg}} + N_{\text{non-}\Lambda_c^+} \cdot f_{\text{non-}\Lambda_c^+}, \quad (1)$$

$$f_{\text{sideband}} = N'_{\text{non-}\Lambda_c^+} \cdot f_{\text{non-}\Lambda_c^+} = h \cdot N_{\text{non-}\Lambda_c^+} \cdot f_{\text{non-}\Lambda_c^+}, \quad (2)$$

where N_{sig} , $N_{\Lambda_c^+ \text{ bkg}}$, and $N_{\text{non-}\Lambda_c^+}$ denote the signal yield, the $\Lambda_c^+ \bar{\Lambda}_c^-$ background yield, and the non- Λ_c^+ background yield in the signal region, $N'_{\text{non-}\Lambda_c^+}$ denotes the non- Λ_c^+ yield in the sideband region. The ratio h between $N'_{\text{non-}\Lambda_c^+}$ and $N_{\text{non-}\Lambda_c^+}$ is fixed to 1.262 by fitting the M_{BC} distribution combined 11 ST modes and calculating the ratio between the number of background events in the sideband region and that of the signal region. This method ensures that the non- Λ_c^+ (or $q\bar{q}$) background is well-estimated and as done in the previous BESIII measurement of $\Lambda_c^+ \rightarrow nK_S^0\pi^+$ [30]. The background from the Λ_c^+ decays, $f_{\Lambda_c^+ \text{ bkg}}$, is described by a shape extracted from the inclusive MC sample. The background from the non- Λ_c^+ decay is modeled as:

$$f_{\text{non-}\Lambda_c^+} = ((1-k) \cdot f_1 + k \cdot f_{K_S^0}) \cdot f_2, \quad (3)$$

where f_1 and f_2 represent the first-order Chebychev polynomials, k is the fraction of the K_S^0 component and free in the fit, and $f_{K_S^0}$ represents the shape of the K_S^0 signal extracted from the signal MC samples which has the same K_S^0 shape as the background process.

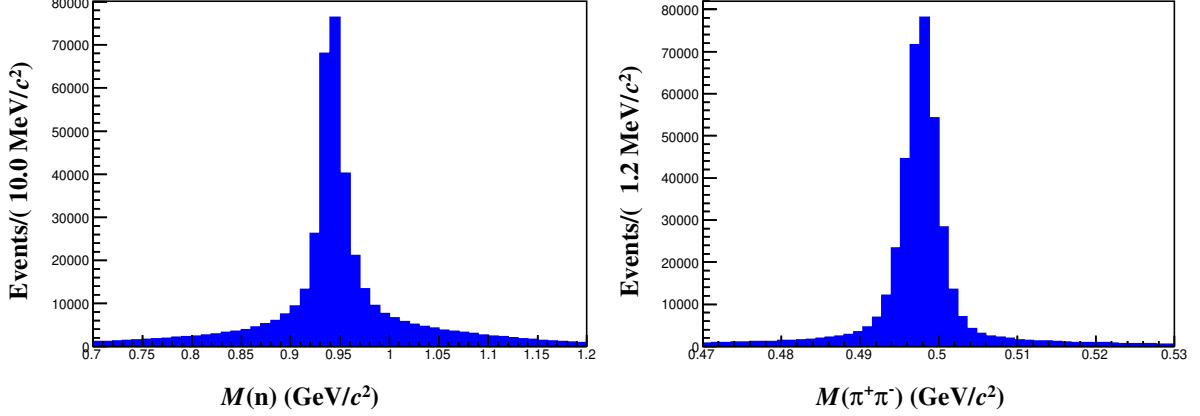


Figure 3. The blue histograms represent $M(n)$ and $M(\pi^+\pi^-)$ distributions of signal MC in the signal region.

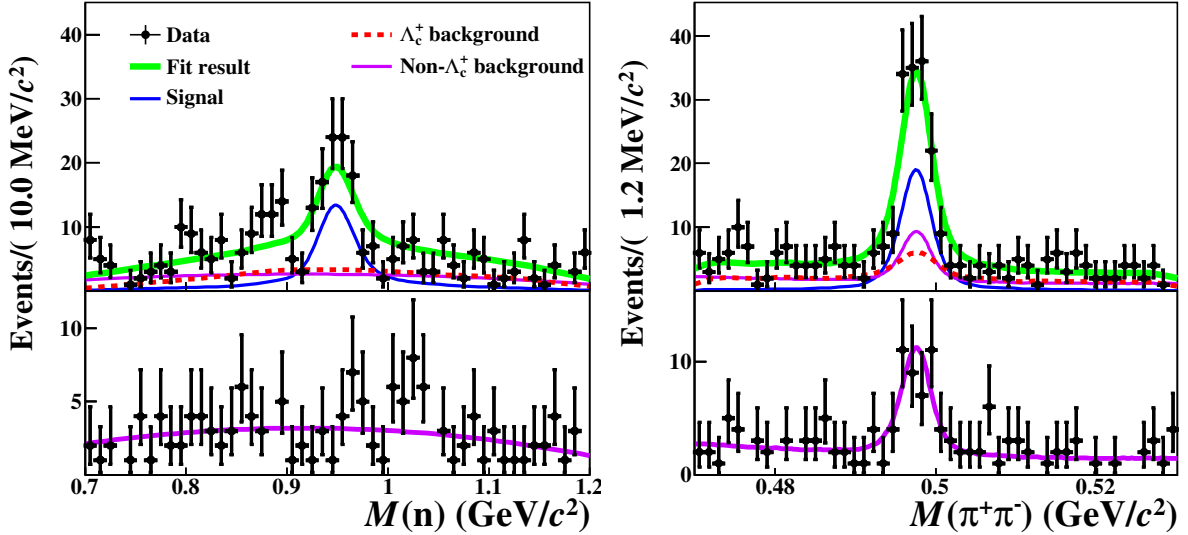


Figure 4. The 2D simultaneous fit on the accepted candidates in the signal (top) and sideband (bottom) regions. The black dots with error bars represent data. The green solid lines represent the total fit results. The blue lines, purple lines, and red dashed lines represent the signal, non- $\Lambda_c^+\Lambda_c^-$ background, and $\Lambda_c^+\Lambda_c^-$ pair decay background, respectively.

Fig. 4 shows the fit results. The total signal yield of $\Lambda_c^+ \rightarrow nK_S^0\pi^+\pi^0$ summing over eleven ST modes and seven c.m. energies is determined to be $N^{\text{DT}} = 98 \pm 15$. The BF of $\Lambda_c^+ \rightarrow nK_S^0\pi^+\pi^0$ is calculated by

$$\mathcal{B} = \frac{N^{\text{DT}}}{\sum_{ij} N_{ij}^{\text{ST}} \cdot (\varepsilon_{ij}^{\text{DT}} / \varepsilon_{ij}^{\text{ST}}) \cdot \mathcal{B}_{\text{int}}}, \quad (4)$$

where the indices i and j are the eleven ST modes and seven c.m. energies, respectively, and \mathcal{B}_{int} are the BFs of $K_S^0 \rightarrow \pi^+\pi^-$ and $\pi^0 \rightarrow \gamma\gamma$ [2]. The DT efficiencies $\varepsilon_{ij}^{\text{DT}}$, ST yields N_{ij}^{ST} , and ST efficiencies $\varepsilon_{ij}^{\text{ST}}$ are listed in Tables II, III, and IV, respectively. The significance considering systematic uncertainty (see below) is evaluated to be 9.2σ via $\sqrt{-2 \times \Delta \ln \mathcal{L}}$, where $\Delta \ln \mathcal{L}$ is the variation in $\ln \mathcal{L}$ of the likelihood fit with and without the signal

component included. Here, the method of considering systematic uncertainty is the same as the systematic uncertainty from fitting model described in the next section, and the minimum significance among all the fitting models is taken as the final significance.

In order to consider potential intermediate resonant states in the decay of $\Lambda_c^+ \rightarrow nK_S^0\pi^+\pi^0$, the distributions of the momenta of the four daughter particles $p(K_S)$, $p(n)$, $p(\pi^0)$, $p(\pi^+)$, and the invariant mass $M(n\pi^+\pi^0)$ are re-weighted according to the data to obtain the DT efficiency. The derivations of the ST yields and ST efficiencies are the same as Ref. [6]. The BF of $\Lambda_c^+ \rightarrow nK_S^0\pi^+\pi^0$ is calculated to be $(0.85 \pm 0.13)\%$, where the uncertainty is statistical only.

Table II. The ST yields, N_{ij}^{ST} , at seven c.m. energies. The uncertainties are statistical only.

Tag mode	4599.53 MeV	4611.86 MeV	4628.00 MeV	4640.91 MeV	4661.24 MeV	4681.92 MeV	4698.82 MeV
$\bar{p}K_S^0$	1243 ± 35	226 ± 15	994 ± 33	1048 ± 34	1044 ± 33	3141 ± 57	889 ± 30
$\bar{p}K^+\pi^-$	6607 ± 89	1094 ± 37	5513 ± 37	5842 ± 83	5447 ± 79	15919 ± 134	4680 ± 73
$\bar{p}K_S^0\pi^0$	587 ± 33	119 ± 16	569 ± 33	552 ± 33	527 ± 32	1591 ± 56	414 ± 30
$\bar{p}K_S^0\pi^-\pi^+$	594 ± 33	100 ± 15	475 ± 30	484 ± 30	487 ± 21	1365 ± 51	414 ± 28
$\bar{p}K^+\pi^-\pi^0$	1965 ± 71	331 ± 30	1453 ± 75	1458 ± 63	1460 ± 63	4361 ± 109	1172 ± 62
$\bar{\Lambda}\pi^-$	738 ± 27	116 ± 11	636 ± 27	664 ± 27	624 ± 26	1916 ± 45	495 ± 23
$\bar{\Lambda}\pi^-\pi^0$	1681 ± 54	281 ± 22	1342 ± 50	1483 ± 50	1338 ± 46	3900 ± 78	1145 ± 43
$\bar{\Lambda}\pi^-\pi^+\pi^-$	744 ± 35	130 ± 14	547 ± 31	690 ± 34	703 ± 33	1847 ± 55	569 ± 31
$\bar{\Sigma}^0\pi^-$	502 ± 25	95 ± 12	384 ± 22	413 ± 23	414 ± 22	1267 ± 38	334 ± 20
$\bar{\Sigma}^-\pi^0$	309 ± 24	68 ± 10	242 ± 21	271 ± 22	264 ± 22	770 ± 38	216 ± 21
$\bar{\Sigma}^-\pi^-\pi^+$	1146 ± 47	204 ± 21	922 ± 19	995 ± 46	949 ± 44	2729 ± 79	848 ± 42

Table III. The ST efficiencies, $\varepsilon_{ij}^{\text{ST}}\%$, at seven c.m. energies. The uncertainties are statistical only. The quoted efficiencies do not include any sub-decay BFs.

Tag mode	4599.53 MeV	4611.86 MeV	4628.00 MeV	4640.91 MeV	4661.24 MeV	4681.92 MeV	4698.82 MeV
$\bar{p}K_S^0$	54.6 ± 0.2	50.8 ± 0.6	48.9 ± 0.2	47.9 ± 0.2	46.4 ± 0.2	45.2 ± 0.1	44.1 ± 0.2
$\bar{p}K^+\pi^-$	49.9 ± 0.1	47.8 ± 0.2	46.1 ± 0.1	45.3 ± 0.1	44.3 ± 0.1	42.8 ± 0.1	41.9 ± 0.1
$\bar{p}K_S^0\pi^0$	22.2 ± 0.2	20.8 ± 0.4	19.2 ± 0.2	19.1 ± 0.2	18.2 ± 0.2	17.6 ± 0.1	16.7 ± 0.2
$\bar{p}K_S^0\pi^-\pi^+$	22.8 ± 0.2	20.4 ± 0.4	19.2 ± 0.2	19.3 ± 0.2	18.3 ± 0.2	18.7 ± 0.1	17.4 ± 0.2
$\bar{p}K^+\pi^-\pi^0$	19.4 ± 0.1	18.1 ± 0.2	16.8 ± 0.1	16.2 ± 0.1	15.7 ± 0.1	15.4 ± 0.0	14.9 ± 0.1
$\bar{\Lambda}\pi^-$	47.1 ± 0.3	44.2 ± 0.6	40.7 ± 0.3	40.2 ± 0.3	38.8 ± 0.3	38.2 ± 0.2	36.2 ± 0.3
$\bar{\Lambda}\pi^-\pi^0$	20.8 ± 0.1	18.4 ± 0.2	17.6 ± 0.1	17.5 ± 0.1	16.9 ± 0.1	16.1 ± 0.1	15.7 ± 0.1
$\bar{\Lambda}\pi^-\pi^+\pi^-$	15.1 ± 0.1	12.7 ± 0.3	12.7 ± 0.1	13.2 ± 0.1	12.7 ± 0.1	12.5 ± 0.1	13.0 ± 0.1
$\bar{\Sigma}^0\pi^-$	28.4 ± 0.2	24.8 ± 0.5	25.3 ± 0.2	24.2 ± 0.2	24.0 ± 0.2	23.2 ± 0.1	21.9 ± 0.2
$\bar{\Sigma}^-\pi^0$	22.8 ± 0.3	21.0 ± 0.6	21.5 ± 0.3	22.3 ± 0.3	20.5 ± 0.3	19.6 ± 0.1	18.3 ± 0.3
$\bar{\Sigma}^-\pi^-\pi^+$	24.5 ± 0.1	23.8 ± 0.3	21.9 ± 0.1	21.6 ± 0.1	20.9 ± 0.1	20.0 ± 0.1	19.9 ± 0.1

Table IV. The DT efficiencies of $\Lambda_c^+ \rightarrow nK_S^0\pi^+\pi^0$, $\varepsilon_{ij}^{\text{DT}}\%$, at seven c.m. energies. The uncertainties are statistical only. The quoted efficiencies do not include any sub-decay BFs.

Tag mode	4599.53 MeV	4611.86 MeV	4628.00 MeV	4640.91 MeV	4661.24 MeV	4681.92 MeV	4698.82 MeV
$\bar{p}K_S^0$	8.3 ± 0.1	8.0 ± 0.1	7.5 ± 0.1	7.0 ± 0.1	6.8 ± 0.1	6.7 ± 0.1	6.5 ± 0.1
$\bar{p}K^+\pi^-$	8.1 ± 0.1	7.3 ± 0.1	7.1 ± 0.1	7.0 ± 0.1	7.0 ± 0.1	6.6 ± 0.2	6.4 ± 0.1
$\bar{p}K_S^0\pi^0$	3.1 ± 0.1	2.9 ± 0.1	2.8 ± 0.1	2.6 ± 0.1	2.7 ± 0.1	2.6 ± 0.1	2.4 ± 0.1
$\bar{p}K_S^0\pi^-\pi^+$	3.0 ± 0.1	2.5 ± 0.1	2.4 ± 0.1	2.4 ± 0.1	2.4 ± 0.1	2.3 ± 0.1	2.3 ± 0.1
$\bar{p}K^+\pi^-\pi^0$	3.1 ± 0.1	2.8 ± 0.1	2.6 ± 0.1	2.6 ± 0.1	2.4 ± 0.1	2.3 ± 0.1	2.3 ± 0.1
$\bar{\Lambda}\pi^-$	7.2 ± 0.1	6.3 ± 0.1	5.9 ± 0.1	5.9 ± 0.1	5.9 ± 0.1	5.5 ± 0.2	5.5 ± 0.1
$\bar{\Lambda}\pi^-\pi^0$	3.0 ± 0.1	2.7 ± 0.1	2.5 ± 0.1	2.3 ± 0.1	2.3 ± 0.1	2.3 ± 0.1	2.3 ± 0.1
$\bar{\Lambda}\pi^-\pi^+\pi^-$	2.0 ± 0.1	1.8 ± 0.1	1.7 ± 0.1	1.7 ± 0.1	1.7 ± 0.1	1.7 ± 0.1	1.7 ± 0.1
$\bar{\Sigma}^0\pi^-$	4.3 ± 0.1	3.8 ± 0.1	3.6 ± 0.1	3.5 ± 0.1	3.5 ± 0.1	3.3 ± 0.1	3.3 ± 0.1
$\bar{\Sigma}^-\pi^0$	3.5 ± 0.1	3.4 ± 0.1	3.2 ± 0.1	3.1 ± 0.1	2.8 ± 0.1	2.7 ± 0.1	2.6 ± 0.1
$\bar{\Sigma}^-\pi^-\pi^+$	3.8 ± 0.1	3.6 ± 0.1	3.4 ± 0.1	3.3 ± 0.1	3.2 ± 0.1	3.0 ± 0.1	2.9 ± 0.1

SYSTEMATIC UNCERTAINTIES

The systematic uncertainties include the π^+ tracking and PID, π^0 and K_S^0 reconstruction, fitting models of tag and signal sides, MC statistics, mass window of peaking backgrounds, and MC model, as summarized in Table V.

The systematic uncertainty from the π^+ tracking and PID is studied by using the control sample $e^+e^- \rightarrow K^+K^-\pi^+\pi^-$. An alternative efficiency is calculated by re-weighting events with momentum-dependent efficiency correction factors extracted from the control sample. The difference between the nominal and alternative efficiencies, 0.3%, is taken as systematic uncertainty.

The systematic uncertainties due to the reconstruction of π^0 and K_S^0 candidates are determined using the control samples $e^+e^- \rightarrow K^+K^-\pi^+\pi^-\pi^0$ and $J/\psi \rightarrow K^*(892)^+K^- \rightarrow K_S^0\pi^+K^-$. The difference of efficiencies between data and MC simulation is estimated with the same method used for π^+ tracking and PID. The systematic uncertainty is estimated to be 0.9% for K_S^0 reconstruction and 0.2% for π^0 reconstruction. The uncertainties of the BFs of $\pi^0 \rightarrow \gamma\gamma$ and $K_S^0 \rightarrow \pi^+\pi^-$, which are quoted from the PDG [2], are 0.03% and 0.1%, respectively.

Uncertainties on the ST yields, DT efficiencies, and ST efficiencies all contribute to systematic uncertainties. The propagated uncertainties, as described by Eq. (4), lead to a total uncertainty of 0.4%.

The uncertainty of 0.2% on the fitting model of the ST side is quoted from Ref. [6]. To estimate the uncertainty of the 2D signal shape in the fit, we use two Gaussian functions to describe the signal contribution and take the difference of the fitted signal yields, 0.6%, as the systematic uncertainty. In the nominal fit, the ratio between $N'_{\text{non-}\Lambda_c^+}$ and $N_{\text{non-}\Lambda_c^+}$, is fixed at 1.262 ± 0.005 . To evaluate the systematic uncertainty from the ratio, it is varied by one standard deviation and the change of the signal yield is less than 0.1%, which is negligible. In the nominal fit, the background shape is exacted from the inclusive MC sample by RooKeysPdf [31]. The uncertainty of the shape of Λ_c^+ background is considered by changing the smoothness factor of the RooKeysPdf from 0 to 1, and the difference of the signal yield, 1.8%, is taken as the systematic uncertainty. Hence, the total systematic uncertainty associated with the fitting model of signal side is 1.9%.

The systematic uncertainty of the peaking background window is estimated by using the control samples of $\Lambda_c^+ \rightarrow \Sigma^+(n\pi^+)\pi^+\pi^-$, $\Sigma^-(n\pi^-)\pi^+\pi^+$, and $\Lambda(n\pi^0)\pi^+$. Gaussian functions are used to describe the difference between data and MC simulation. Using the simulated shapes convolved with Gaussian functions to fit the distributions of $M(n\pi^+)$, $M(n\pi^-)$, and $M(n\pi^0)$, the parameters of the Gaussian functions are determined. The signal MC samples are smeared based on the widths

and means of these Gaussian functions. The difference of the fitted signal yield, 0.3%, is taken as the systematic uncertainty.

The nominal DT efficiencies are calculated by weighting the signal MC samples. The efficiency difference between the weighted and PHSP signal MC samples, 3.0%, is taken as the systematic uncertainty.

The total systematic uncertainty, 3.7%, is obtained via the quadrature sum of the individual components.

Table V. Systematic uncertainties in the BF measurement.

Source	$\Lambda_c^+ \rightarrow nK_S^0\pi^+\pi^0$ (%)
π^+ tracking and PID	0.3
π^0 reconstruction	0.2
K_S^0 reconstruction	0.9
$\mathcal{B}(K_S^0 \rightarrow \pi^+\pi^-)$	0.1
MC statistics	0.4
Fitting model of tag side	0.2
Fitting model of signal side	1.9
Peaking background window	0.3
MC model	3.0
Total	3.7

SUMMARY

In summary, based on 4.5 fb^{-1} of e^+e^- collision data samples taken at c.m. energies between 4599.53 MeV and 4698.82 MeV with the BESIII detector, the BF of $\Lambda_c^+ \rightarrow nK_S^0\pi^+\pi^0$ is measured to be $(0.85 \pm 0.13 \pm 0.03)\%$, with a significance of 9.2σ , where the first uncertainty is statistical and the second systematic. Table VI summarizes the BFs of $\Lambda_c^+ \rightarrow nK_S^0\pi^+\pi^0$ and its isospin partners. The measured BF differs with the prediction of isospin statistical model [12], $(1.54 \pm 0.08)\%$ by 4.4 σ . This indicates that there may be resonant contributions or some unknown dynamics in this decay. The total BF of the four body decay $\Lambda_c^+ \rightarrow N\bar{K}\pi\pi$ is predicted to be $(12.88 \pm 0.69)\%$ [12]. Our BF, together with the BFs of its isospin partners, offer important constraint on the theoretical prediction.

Table VI. The BFs of $\Lambda_c^+ \rightarrow nK_S^0\pi^+\pi^0$ and its isospin partners.

Decay mode	BF ($\times 10^{-2}$)
$\Lambda_c^+ \rightarrow pK^-\pi^+\pi^0$	4.53 ± 0.38 [5]
$\Lambda_c^+ \rightarrow nK^-\pi^+\pi^+$	1.90 ± 0.12 [6]
$\Lambda_c^+ \rightarrow pK_S^0\pi^+\pi^-$	1.53 ± 0.14 [5]
$\Lambda_c^+ \rightarrow nK_S^0\pi^+\pi^0$ (Theoretical prediction)	1.54 ± 0.08 [12]
$\Lambda_c^+ \rightarrow nK_S^0\pi^+\pi^0$ (This work)	$0.85 \pm 0.13 \pm 0.03$

ACKNOWLEDGMENTS

The BESIII Collaboration thanks the staff of BEPCII and the IHEP computing center for their strong support. This work is supported in part by National Key R&D Program of China under Contracts Nos. 2020YFA0406400, 2020YFA0406300; National Natural Science Foundation of China (NSFC) under Contracts Nos. 12375070, 11635010, 11735014, 11835012, 11935015, 11935016, 11935018, 11961141012, 12025502, 12035009, 12035013, 12061131003, 12192260, 12192261, 12192262, 12192263, 12192264, 12192265, 12221005, 12225509, 12235017; the Chinese Academy of Sciences (CAS) Large-Scale Scientific Facility Program; the CAS Center for Excellence in Particle Physics (CCEPP); Joint Large-Scale Scientific Facility Funds of the NSFC and CAS under Contract No. U2032108, No. U1832207; CAS Key Research Program of Frontier Sciences under Contracts Nos. QYZDJ-SSW-SLH003, QYZDJ-SSW-SLH040; 100 Talents Program of CAS; Fundamental Research Funds for the Central Universities, Lanzhou University, University of Chinese Academy of Sciences; The Institute of Nuclear and Particle Physics (INPAC) and Shanghai Key Laboratory for Particle Physics and Cosmology; European Union's Horizon 2020 research and innovation programme under Marie Skłodowska-Curie grant agreement under Contract No. 894790; German Research Foundation DFG under Contracts Nos. 455635585, Collaborative Research Center CRC 1044, FOR5327, GRK 2149; Istituto Nazionale di Fisica Nucleare, Italy; Ministry of Development of Turkey under Contract No. DPT2006K-120470; National Research Foundation of Korea under Contract No. NRF-2022R1A2C1092335; National Science and Technology fund of Mongolia; National Science Research and Innovation Fund (NSRF) via the Program Management Unit for Human Resources & Institutional Development, Research and Innovation of Thailand under Contract No. B16F640076; Polish National Science Centre under Contract No. 2019/35/O/ST2/02907; The Swedish Research Council; U. S. Department of Energy under Contract No. DE-FG02-05ER41374.

[1] G. S. Abrams *et al.* *Phys. Rev. Lett.* **44**, 10 (1980).
 [2] R. L. Workman *et al.* (Particle Data Group), *PTEP* **2022**, 083C01 (2022).
 [3] H. B. Li and X. R. Lyu, *Natl. Sci. Rev.* **8** (2021), nwab181.
 [4] M. Ablikim *et al.* (BESIII Collaboration), *Phys. Rev. D* **108**, L031101 (2023).

[5] M. Ablikim *et al.* (BESIII Collaboration), *Phys. Rev. Lett.* **116**, 052001 (2016).
 [6] M. Ablikim *et al.* (BESIII Collaboration), *Chin. Phys. C* **47**, 023001 (2023).
 [7] L. L. Chau and H. Y. Cheng, *Phys. Rev. Lett.* **56**, 1655 (1986).
 [8] L. L. Chau, H. Y. Cheng and B. Tseng, *Phys. Rev. D* **54**, 2132 (1996).
 [9] M. Bauer, B. Stech and M. Wirbel, *Z. Phys. C* **34**, 103 (1987).
 [10] H. Y. Cheng and B. Tseng, *Phys. Rev. D* **48**, 4188 (1993).
 [11] H. Y. Cheng, *Chin. J. Phys.* **78**, 324 (2022).
 [12] M. Gronau and J. L. Rosner, *Phys. Rev. D* **97**, 116015 (2018).
 [13] M. Ablikim *et al.* (BESIII Collaboration), *Chin. Phys. C* **40**, 063001 (2016).
 [14] M. Ablikim *et al.* (BESIII Collaboration), *Chin. Phys. C* **46**, 113002 (2022).
 [15] M. Ablikim *et al.* (BESIII Collaboration), *Chin. Phys. C* **46**, 113003 (2022).
 [16] B. C. Ke, J. Koponen, H. B. Li and Y. Zheng, *Ann. Rev. Nucl. Part. Sci.* **73**, 285 (2023).
 [17] R. M. Baltrusaitis *et al.* (MARK-III Collaboration), *Phys. Rev. Lett.* **56**, 2140 (1986); J. Adler *et al.* (MARK-III Collaboration), *Phys. Rev. Lett.* **60**, 89 (1988).
 [18] M. Ablikim *et al.* (BESIII Collaboration), *Nucl. Instrum. Meth. A* **614**, 345 (2010).
 [19] C. Yu, Z. Duan, S. Gu, Y. Guo, X. Huang, D. Ji, H. Ji, Y. Jiao, Z. Liu and Y. Peng, *et al.*, *Proceedings of IPAC2016, Busan, Korea*.
 [20] M. Ablikim *et al.* (BESIII Collaboration), *Chin. Phys. C* **44**, 040001 (2020).
 [21] S. Agostinelli *et al.* (GEANT4 Collaboration), *Nucl. Instrum. Meth. A* **506**, 250 (2003); J. Allison *et al.*, *IEEE Trans. Nucl. Sci.* **53**, 270 (2006); J. Allison *et al.*, *Nucl. Instrum. Meth. A* **835**, 186 (2016).
 [22] K. X. Huang, *et al.*, *Nucl. Sci. Tech.* **33**, 142 (2022).
 [23] S. Jadach, B. F. L. Ward and Z. Was, *Comp. Phys. Commu.* **130**, 260 (2000); *Phys. Rev. D* **63**, 113009 (2001).
 [24] E. Barberio, B. van Eijk and Z. Was, *Comput. Phys. Commun.* **66**, 115 (1991); E. Richter-Was, *Phys. Lett. B* **303**, 163 (1993); P. Golonka and Z. Was, *Eur. Phys. J. C* **45**, 97 (2006).
 [25] R. G. Ping, *Chin. Phys. C* **32**, 599 (2008).
 [26] D. J. Lange, *Nucl. Instrum. Meth. A* **462**, 152 (2001).
 [27] J. C. Chen, G. S. Huang, X. R. Qi, D. H. Zhang and Y. S. Zhu, *Phys. Rev. D* **62**, 034003 (2000); R. L. Yang, R. G. Ping and H. Chen, *Chin. Phys. Lett.* **31**, 061301 (2014).
 [28] R. L. Yang, R. G. Ping and H. Chen, *Chin. Phys. Lett.* **31**, 061301 (2014).
 [29] M. Ablikim *et al.* (BESIII Collaboration), *Phys. Rev. Lett.* **131**, 191901 (2023).
 [30] M. Ablikim *et al.* (BESIII Collaboration), *Phys. Rev. Lett.* **118**, 112001 (2017).
 [31] K. S. Cranmer, *Comput. Phys. Commun.* **136**, 198-207 (2001).